Carcinogenesis, 2020, Vol. 41, No. 1, 100–110

doi:10.1093/carcin/bgz169
Advance Access Publication October 5, 2019
Original Article

ORIGINAL ARTICLE

Multiple myeloma BM-MSCs increase the tumorigenicity of MM cells via transfer of VLA4-enriched microvesicles

Mahmoud Dabbah[1,6], Osnat Jarchowsky-Dolberg[2,6], Oshrat Attar-Schneider[1,3], Shelly Tartakover Matalon[1,6], Metsada Pasmanik-Chor[5], Liat Drucker[1,6,*,†] and Michael Lishner[1,2,4,6,†]

[1]Oncogenetic Laboratory, [2]Hematology Unit, [3]Lung Cancer Research Laboratory, and [4]Research Institute, Meir Medical Center, Kfar Saba, [5]Bioinformatics Unit, G.S.W. Faculty of Life Sciences, [6]Sackler Faculty of Medicine, Tel Aviv University, Tel Aviv, Israel

*To whom correspondence should be addressed. Tel: +972-9-7472466; Fax: +972-9-7471145; Email: druckerl@clalit.org.il
†These authors contributed equally to this study.

Abstract

Multiple myeloma (MM) cells accumulate in the bone marrow (BM) where their interactions impede disease therapy. We have shown that microvesicles (MVs) derived from BM mesenchymal stem cells (MSCs) of MM patients promote the malignant traits via modulation of translation initiation (TI), whereas MVs from normal donors (ND) do not. Here, we observed that this phenomenon is contingent on a MVs' protein constituent, and determined correlations between the MVs from the tumor microenvironment, for example, MM BM-MSCs and patients' clinical characteristics. BM-MSCs' MVs (ND/MM) proteomes were assayed (mass spectrometry) and compared. Elevated integrin CD49d (X80) and CD29 (X2) was determined in MM-MSCs' MVs and correlated with patients' staging and treatment response (free light chain, BM plasma cells count, stage, response to treatment). BM-MSCs' MVs uptake into MM cell lines was assayed (flow cytometry) with/without integrin inhibitors (RGD, natalizumab, and anti-CD29 monoclonal antibody) and recipient cells were analyzed for cell count, migration, MAPKs, TI, and drug response (doxorubicin, Velcade). Their inhibition, particularly together, attenuated the uptake of MM-MSCs MVs (but not ND-MSCs MVs) into MM cells and reduced MM cells' signaling, phenotype, and increased drug response. This study exposed a critical novel role for CD49d/CD29 on MM-MSCs MVs and presented a discriminate method to inhibit cancer promoting action of MM-MSCs MVs while retaining the anticancer function of ND-MSCs-MVs. Moreover, these findings demonstrate yet again the intricacy of the microenvironment involvement in the malignant process and highlight new therapeutic avenues to be explored.

Introduction

Multiple myeloma (MM) is characterized with the accumulation of malignant plasma cells in the bone marrow (BM) (1,2). Many of MM genetic aberrations can already be detected in its precursor states of monoclonal gammopathy of undetermined significance (MGUS) and smoldering multiple myeloma (SMM) (1). This observation underscores a significant role for the BM niche and epigenetic influences in disease progression (3,4). Indeed, it is well established that the BM microenvironment is a critical driver of MM progression and an obstacle to effective treatment (5,6). Despite this recognition, the mechanisms underlying the permissive microenvironment are far from identified emphasizing the need for better understanding in order to implement more effective treatment.

The BM niche consists of multiple cell types primarily produced from hematopoietic stem cells (lymphoid and myeloid) or mesenchymal stem cells (MSCs) (stroma), extracellular matrix (ECM), microvesicles (MVs), and solubles (5,6). In a series of publications, we have shown that the BM-MSCs affect MM according

Received: April 30 2019; **Revised:** September 16 2019; **Accepted:** October 2 2019

Abbreviations

BM-MSCs	bone marrow mesenchymal stem cells
Dox	doxorubicin
eIF4E	eukaryotic translation initiation factor 4E
eIF4GI	eukaryotic translation initiation factor 4GI
MM	multiple myeloma
MM-MSCs	multiple myeloma mesenchymal stem cells
MVs	microvesicles
ND-MSCs	normal donor mesenchymal stem cells
NTZ	natalizumab
TI	translation initiation
Vel	Velcade

to their normal or pathological source (7–9). Specifically, we have demonstrated that MSCs from MM patients' BM aspirates (MM-MSCs) promote the proliferation and migration of MM cells via MAPKs/translation initiation (TI) signaling cascades. On the contrary, BM-MSCs from normal donors (ND-MSCs) do not stimulate MAPKs/TI/proliferation and migration (7). These observations show unequivocally that the BM-MSCs of MM patients differ from the BM-MSCs of ND.

In search of communication routes between the BM-MSCs and the MM cells, we assayed their secreted microvesicles (MVs) (8,10,11). Since MVs are produced by fission from the cells' membranes they hold resemblance to their source and transfer membrane embedded molecules as well as internal cytoplasmic cargoes to their target cells (12,13). A growing body of evidence shows that the uptake of MVs functions as a significant means of crosstalk capable of modulating recipient cells' characteristics (10,14,15). Concordantly, we have also observed that ND and MM-MSCs MVs differentially affect MM cells signaling and phenotype with suppressive or promotive influences, respectively, and in parallel to the effects of whole BM-MSCs (7,8). We assumed that the MVs cargoes are responsible for their variance in function and its characterization was an aim in this study. We also conjectured that comparing the MVs cargoes with their effect on MM cells may yield markers for the microenvironment's contribution to MM progression and possibly afford novel therapeutic targets.

Interestingly, BM-MSCs MVs were able to activate MAPKs before the uptake of the vesicles (8) so we hypothesized that a membranal constituent is responsible for this immediate signal and such a component may be a protein. Moreover, this observation suggested it may be possible to selectively prevent the uptake of MM-MSCs MVs altogether and became a major objective in our research.

In the current study, we explored the protein cargo by high-throughput mass spectrometry analysis of the BM-MSCs MVs (ND, MM). In support of our work hypothesis, we determined differences between the MM-MSCs and ND-MSCs' MVs proteomes, with distinct changes in membranal proteins, clinically correlated with MM staging and response to therapy. We also present a way to selectively control of MM-MSCs MVs' uptake and improve drug response.

Materials and methods

Cell lines

Each experiment was conducted with freshly defrosted authenticated U266, MM1S, and RPMI 8226 as previously described (16–18). All cell lines' identity was authenticated by STR and routinely screened for mycoplasma absence. U266 and RPMI 8226 (ATCC) were authenticated (STR of 15 loci, 2014) by Genomics Core Facility of BioRap Technologies and the Rappaport Research Institute, Technion, Israel. Authenticated MM1S were obtained from Karin Joehrer lab, Austria (authenticated by STR of 15 loci, 2015). All cell lines were propagated upon receipt/authentication and frozen (80°C) in aliquots.

BM-MSCs isolation and propagation

BM samples were obtained from femur head BM samples of consecutive normal donors (ND), undergoing elective full hip replacement surgery ($n = 15$) and MM patients' BM aspirates taken for medical purposes ($n = 10$) at Meir Medical Center, Israel. All participants signed informed consent forms approved by Meir Medical Center Helsinki Committee. MSCs were isolated from BM samples on a Ficoll gradient and seeded in flask at 40 000 cells/cm^2 with RPMI 1640 supplemented with 10% FBS (Biological Industries). Nonadherent cells were removed with the medium within the first 10 days of culture, leaving the adhered MSCs in the culture dish. Media were replaced twice weekly until the culture was nearly confluent (2–3 weeks); at which time, the cells were harvested for identity validation (vimentin+, keratin, CD271+, CD34, CD45) (immunocytochemistry, flow cytometry (FACS)). The cells were also assayed for their ability to differentiate into adipocytes and osteocytes (16–18).

Microvesicles isolation and application to MM cell lines

Microvesicles (MVs) were isolated from conditioned media collected from 80% confluent BM-MSCs cultures (2–6 weeks) (18). Briefly, media were obtained after cell removal by centrifugation at 800*g* for 5 min and then centrifuged at 4500*g* for 5 min to discard large debris. After centrifugation twice at 20 000*g* (Beckman Ti70 rotor; Beckman Coulter) for 60 min at 4°C, the microvesicles were washed and resuspended in PBS. Isolated BM-MSCs' microvesicles were characterized by size and external expression of phosphatidylserine (electron microscope; Annexin V, FACS) (Supplementary Figure 2, available at *Carcinogenesis* Online), as described by us previously (8). Microvesicles' total protein concentration was determined. The dose of 50 µg/ml BM-MSCs MVs (ND, MM) per 100,000 cells (MM) was chosen as the optimal concentration for the study according to calibrations performed by us previously. This working concentration is also compatible with experimental conditions used by others (8).

Flow cytometry (FACS)

BM-MSCs MVs were identified by size and validated by Annexin binding to exposed phosphatidylserine. MVs uptake into the MM cells was assayed by staining them with the PKH67 dye, according to the manufacturer's instructions (Sigma-Aldrich), and incubating them with MM cells. Then, cells were washed (PBS) and fluorescence was analyzed by FACS (Navios Flow Cytometer, Beckman Coulter). To test the expression levels of CD49d and B1 integrin, 5 µl of each antibody (CD49d-APC Beckman Coulter; integrin B1 P5D2 Santa Cruz) were added to the cells/MVs for 15 min; fluorescence was analyzed (FACS).

MM BM mononuclear cells were separated using Ficoll, cultured and treated with ND/MM PKH67 fluorescent MVs (FITC) with or without uptake inhibitors. Plasma cells (PCs) were gated using 5 µl of each antibody CD38 and CD138-PE (Beckman Coulter), and their MVs uptake was measured using FACS as described above.

Proteomics analysis

MM and ND MSCs microvesicles ($n = 5$ each) were assayed for protein content (analytical proteomics) by mass spectrometry at the Smoler Protein Research Center (Technion). Initial analysis was performed using Perseus (19). Validation of select targets was done by immunoblotting and flow cytometry (Supplementary Figure 3, available at *Carcinogenesis* Online).

Bioinformatics analysis

Mass spectrometry results were analyzed by the Bioinformatics unit at Tel-Aviv University. Log LFQ intensities resulting from Perseus software were statistically analyzed for differentially expressed proteins (ND-MSCs MVs versus MM-MSCs MVs; $P < 0.05$ and FC > 1.75) using Partek Genomics suite (v 6.6; http://www.partek.com/pgs). Differentially expressed protein lists were analyzed for enriched gene ontology and pathways using three different bioinformatics tools (Webgestalt, Gorilla, and ToppGene) (20–22).

Differentially expressed proteins (unique) and ≥1.75 elevated (ND versus MM) from the common proteins in the ND and MM MVs lists were investigated for enriched interesting metabolic pathways and biological process with focus on possible involvement in the MVs-MM cells initial interaction and signaling. Membrane proteins in each MVs cargo were identified by using the bioinformatics function enrichment software David (23).

Trypan blue

Total, viable, and dead cell counts were assayed by Trypan blue dye. Cells were automatically counted by Countess (Invitrogen) (16–18).

Cell viability assay

Cell viability was assayed with cell proliferation reagent WST-1 (Roche, Basel, Switzerland) as described before (16–18).

Western blotting

Proteins lysates were immunoblotted as we described previously (16–18) using rabbit/mouse anti-human: peIF4E (Ser209), peIF4GI (Ser1108), pmTOR (Ser2448), pERK1/2, pJNK, Histone H3, Smad5, Calnexin, HSP90, LMNB1, GPX1, Col1α, and MMP9 (Cell Signaling Technology, Danvers, MA); tubulin (Sigma); NFKB p50 (SC-8414).

Transwell assay

In total, 100,000 MM cells were cultured in the upper chamber of Transwell plate 8.0 μm (corning) with RPMI 3% FBS. The lower chamber contained fibronectin (human plasma, Sigma, 20 μM) dissolved in RPMI 10% FBS, as done previously by others and us (8). BM-MSCs' MVs were added to the cells in the upper chamber. Migrated cells present in the lower chamber were enumerated after 24 h (Countess).

Inhibitors and drugs

MM cells were treated with 166 μM RGD (ANASPEC) for 1.5 and 24 h as published previously (24,25). Natalizumab (Tysabri; 300 mg ampule) was tested for dose response (Figure 4c) and applied to cells at 15 μg/ml for 1.5, 4, and 24 h before analysis. B1 blocker (P5D2 Santa Cruz) was used as indicated by manufacturer at 20 μg/ml. Velcade (bortezomib; CAS179324-69-7) and doxorubicin (TEVA) were obtained from Meir Medical Center pharmacy and used at working concentrations of 5 nM and 1 μM, respectively, as previously (26–28).

Statistical analysis

All experiments were conducted at least three separate times. Student's paired *t*-tests were applied in the analyses of differences between two cohorts. For more than two cohorts, we used the multivariate One-Way-ANOVA test or Kruskal–Wallis nonparametric test, with Bonferroni correction, each when appropriate. An effect was considered significant when *P*-value was less than 0.05. The correlation between CD49d and the MM clinical markers in 19 MM patients was performed using Pearson or Spearman's rho correlations for normal or non-normal distributions, respectively. Tests of normality were performed for all the MM clinical markers data using Kolmogorov–Smirnov and Shapiro–Wilk tests. All statistical analyses were done using SPSS-25 software.

Results

ND and MM-MSCs MVs proteomes display distinct differences

High-throughput unbiased analysis of the BM-MSCs MVs' protein content was carried out by analytical mass spectrometry and results were processed using Bioinformatics tools. Comparison of ND-MSCs MVs and MM-MSCs MVs protein lists (n = 5 each) yielded the immediate observation that there are proteins uniquely expressed in each population and that the commonly expressed proteins may vary significantly in quantity (Figure 1a). In order to further confirm the relevance of our proteomics analysis, we tested the expression of several targets by immunoblotting or flow cytometry (n = 11). To our satisfaction, our analyses corresponded with elevated expression (CD49d, ITGB1, Col 1α, HSP90, HISH3, CD38, and CD9), equal levels (calnexin), and unique expressions (GPX1, MMP9, LMNB1, and CD36) of multiple targets (Supplementary Figure 3, available at *Carcinogenesis* Online) and proved the mass spectrometry data reliable and valid for additional studies. Gene ontology (GO) analyses of the cargo protein lists in BM-MSCs MVs demonstrated fundamental differences in highlighted pathways according to source with three different Bioinformatics tools (Webgestalt, ToppGene, Gorilla) (Table 1). Specifically, ND-MSCs MVs carried proteins implicated in cellular and immune responses to stimuli (18%), ATP synthesis (18%), extracellular matrix (ECM) design and binding (28%), metabolism and mechanisms of cellular uptake (20%). On the contrary, MM-MSCs MVs were enriched with proteins associated with protein translation (50%) and immune response (34%) of annotated pathways (ToppGene) (Figure 1b). These distinct differences between ND and MM-MSCs MVs cargoes are consistent with the variance in their effect on MM cells described by us previously (8). Importantly, the capability of MM-MSCs MVs to modulate translation cascades in recipient MM cells underscores their capacity to design the cells characteristics and promote disease.

Externally expressed proteins are involved in BM-MSCs MVs uptake and signaling

Since we have previously detected that the BM-MSCs MVs activate signaling in recipient MM cells prior any significant MVs uptake, we were particularly interested in proteins situated on the external face of the MVs capable of initial and immediate contact. Therefore, we used two in vitro methods and mildly denaturated proteins epitopes on BM-MSCs MVs (65°C) or digested protruding proteins with trypsin and then tested MVs' uptake into MM cells (Supplementary Figure 1a, available at *Carcinogenesis* Online). While both treatments decreased the BM-MSCs MVs' uptake into the MM cells (U266 and RPMI8226) (↓10–30%, $P < 0.05$) the effect was significantly greater with MM-MSCs MVs compared to ND MSCs-MVs (↑~50%, $P < 0.05$) (Supplementary Figure 1b, available at *Carcinogenesis* Online). We also tested the effect of the mild denaturation on MM-MSCs MVs induced MM cells' proliferation and underlying activation of TI factors eIF4E, eIF4GI, and representative targets (NFκB and SMAD5, respectively). This was done only on MM cells treated with MM-MSCs MVs because we have shown previously that they alone increase the MM cells TI, whereas ND-MSCs MVs decrease TI as (8). Again, we registered no effect on MM cells with the heated MVs (Supplementary Figure 1c–e, available at *Carcinogenesis* Online). Of note, the relative decrease in cell count and TI of denatured MM-MSCs MVs recipient MM cells was greater than the relative decrease in the MVs uptake. This observation may be reconciled by the possible abrogation of the membranal signaling of the vesicles as well, an aspect untested in our model.

Using the function enrichment tool DAVID, we identified proteins capable of expression on the external side of plasma membranes in the BM-MSCs MVs proteomes (Bonferroni p = 8.5E14) (GO: 0009897). A total of 49 proteins expressed on BM-MSCs MVs were identified. Of these proteins, 42 (86%) are common to both ND and MM-MSCs MVs, 4 are unique to ND-MSCs MVs, and 3 exclusively expressed on MM-MSCs MVs (Supplementary Figure 1c, available at *Carcinogenesis* Online).

Integrins facilitate MM-MSCs MVs uptake and membranal signaling in MM cells

One of the major adhesion molecules' families often aberrantly expressed in cancer that may be implicated in MVs uptake are

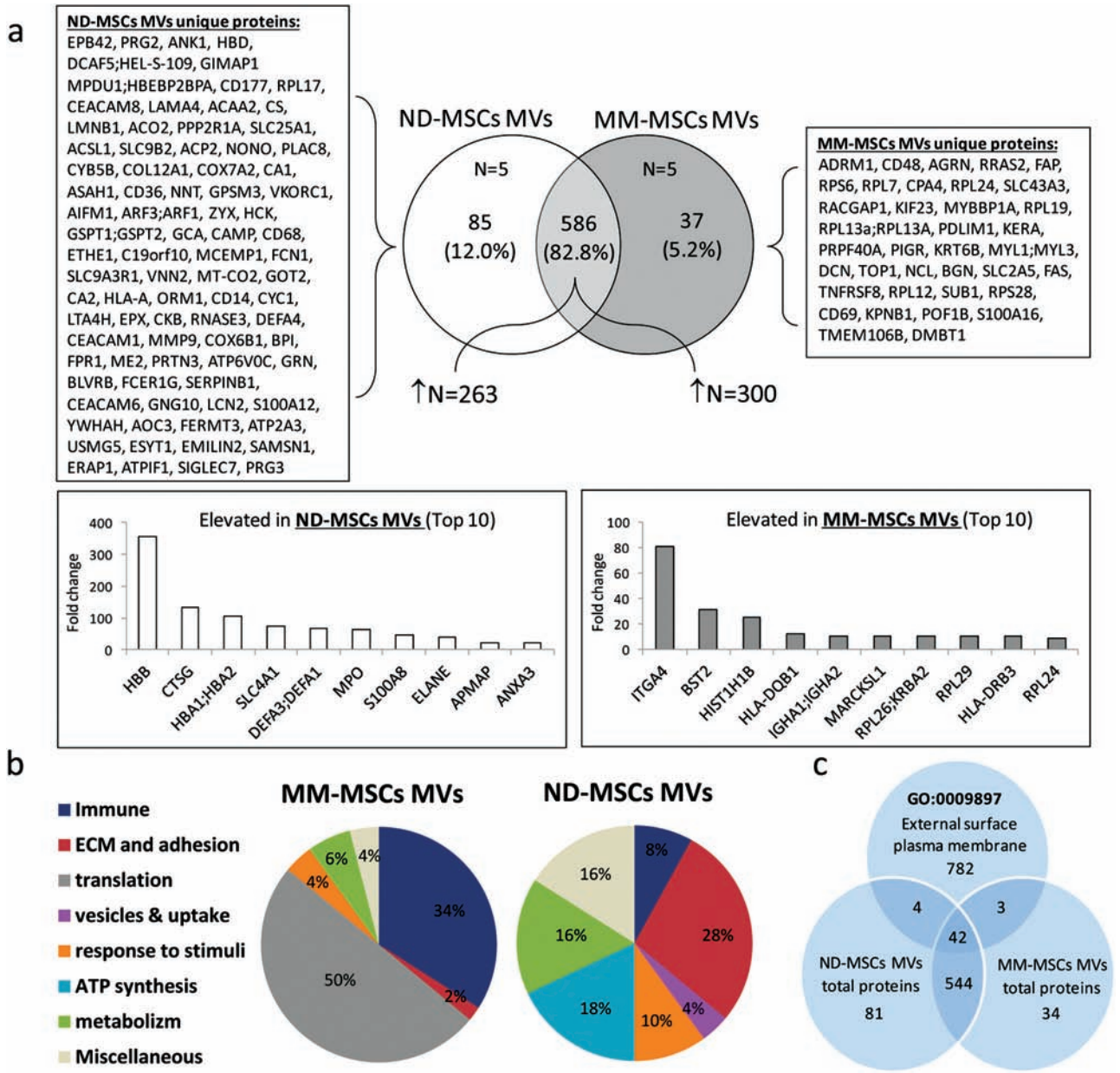

Figure 1. Venn diagram of total BM-MSCs microvesicles proteome and gene ontology (GO) for enrichment pathways and biological process according to their source (ND and MM) ($n = 5$). Protein cargo was characterized by mass spectrometry. (**a**) Unique proteins are listed (left and right panels); the number of the top elevated proteins from the common lest are indicated in the bottom of the Venn diagram, relative top 10 proteins from each MVs source are presented in bottom panels. (**b**) The BM-MSCs MVs mass spectrometry data was assessed for biological process and pathways using GO enrichment tools (ToppGene); top enriched pathways were chosen to demonstrate the differences between ND and MM MSCs cargo. The percentage of GO pathways involved in the biological processes is indicated in the pie chart. All indicated pathways were significant (ND $p.v < 10^{-3}$, Bonferroni). (**c**) DAVID function enrichment tool was used to identify MVs proteins potentially localized on the external membrane cell domain. Venn diagram was applied to describe total BM-MSCs proteins expression numbers on cell surface according to source (ND versus MM).

the integrins (29,30). Interestingly, the protein most elevated on MM-MSCs MVs was integrin α4 (CD49d; ×80 folds) (Figure 1). Moreover, 10 of the external plasma membrane proteins expressed on the BM-MSCs MVs (ND and MM) were integrins (Supplementary Table 1, available at *Carcinogenesis* Online). Hence, it was only natural that first we tested whether integrins are involved in BM-MSCs MVs uptake into MM cells, specifically the biggest subfamily of Arg-Gly-Asp (RGD) receptors (31). Indeed, by inhibiting the binding of RGD integrins expressed on MVs or MM cells with synthetic tripeptide (RGD) we prevented the MVs uptake into the MM cells as well as exposed a significant difference in the uptake mechanism of MVs from ND-MSCs and those secreted from MM-MSCs (Figure 2). Explicitly, RGD inhibited the uptake of MM-MSCs MVs into MM cells (↓22–45%, $P < 0.05$), whereas it had no effect on the uptake of ND-MSCs MVs (NS) (Figure 2a). Of note, the Arg-Gly-Glu (RGE) control did not affect the MM-MSCs MVs uptake. The significance of blocking the RGD-dependent contact/uptake of the MM-MSCs MVs and MM cell lines was further demonstrated in the inhibition of downstream signaling compared to MM cells treated with RGD only (MAPKs and TI status; ↓35–50%, $P < 0.05$) (Figure 2b,c) and cells' migration (↓45–70%, $P < 0.05$) (Figure 2d). The profound reduction

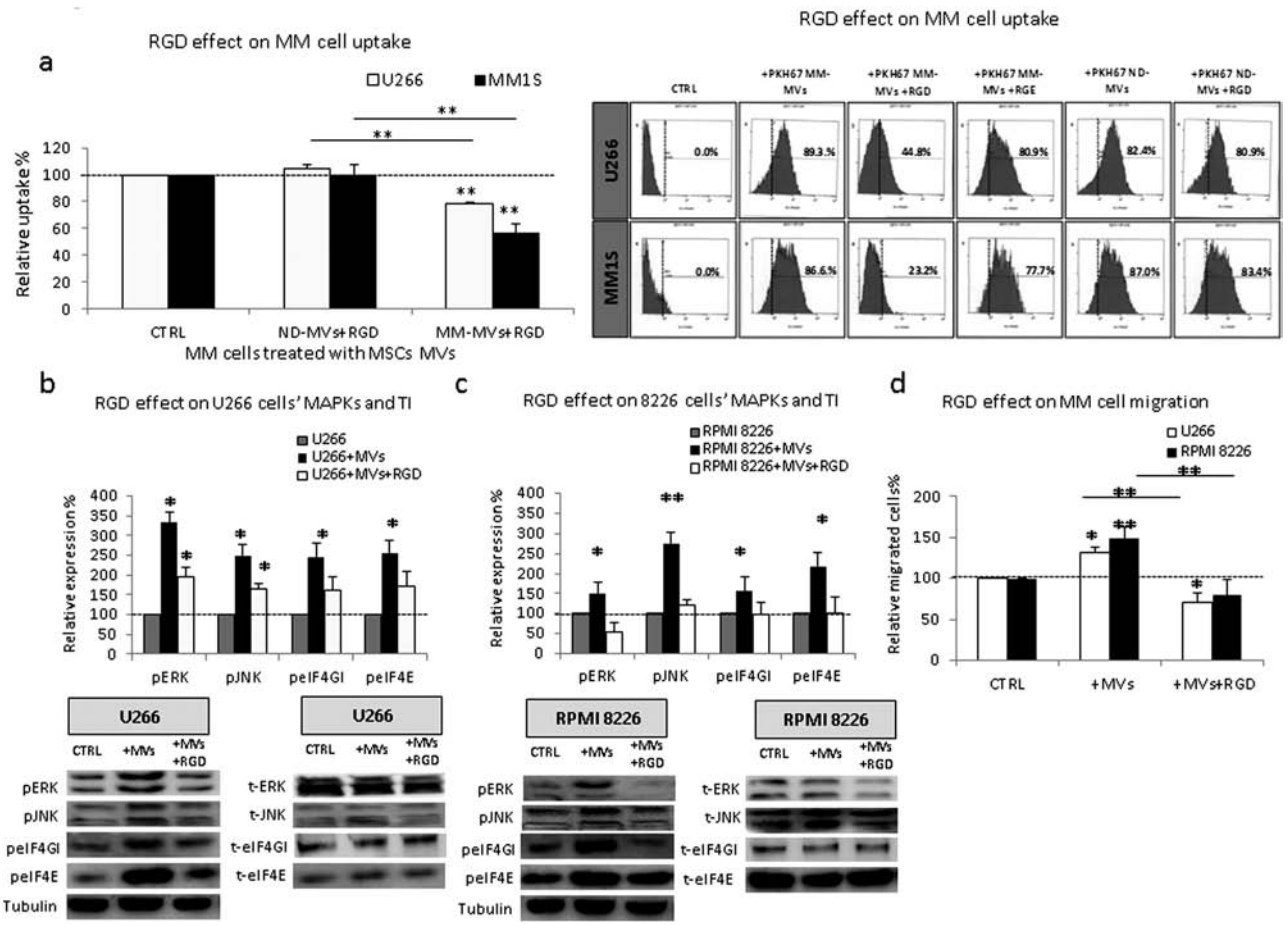

Figure 2. RGD inhibits MM-MSCs effect on MM cell uptake, MAPKs, TI factors, and migration: BM-MSCs MVs (ND/MM) stained with PKH67 were added to MM cells (U266, MM1S) with or without RGD (166 μM). Then, their uptake into MM cells was measured (24 h, FACs. Representative FACS graphs are presented) (**a**). The PKH67 stained MVs' (ND, MM) uptake into untreated MM cells averaged on 95% of the cells and set as the 100% control of the experiment (marked CTRL in (a) section of the figure). Protein lysates were extracted from U266 and RPMI 8266 treated with RGD and MM-MSCs MVs and assayed for p/t eIF4E, p/t eIF4GI, p/t ERK, and p/t JNK (immunoblotting) (**b**, **c**) Results are presented in graphs (top) and representative immunoblots (bottom). All immunoblots were quantified and normalized for tubulin. Results expressed as percent (mean ± SE, $n \geq 3$) of respective protein expression in control cells not treated with MVs and RGD (dotted line). The effect of MM-MSCs MVs on MM cells (U266 and RPMI 8226) migration with or without RGD was tested after 16 h (transwell assay) (**d**) Asterisks depict statistical significance (*$P < 0.05$, **$P < 0.01$).

in MAPKs/TI phosphorylation despite a 30% inhibition of MVs uptake is consistent with our previous observations that the MVs initiate an immediate signal upon contact (prior internalization and cargo uptake) that is also inhibited by the RGD (8). Finally, since identical MM cells responded differently to the ND/MM-MSCs MVs, we deduced that the variance must be attributed to the MVs characteristics and/or their interaction with the cells. Specifically, the proteomic analysis and the use of RGD exposed the significance of different integrins' repertoire on the BM-MSCs MVs in accordance with their source (MM, ND) to their uptake into the malignant cells.

CD49d facilitates the selective MM-MSCs MVs' uptake, signaling, and phenotype design of MM cells

Encouraged by the data demonstrating a role for RGD-dependent integrins in the communication between MM-MSCs MVs and MM cells, we set out to examine the involvement of the highly expressed CD49d. Interestingly, CD49d is already recognized as a negative prognostic marker in MM, overexpressed on minimal residual disease subclones (32), and implicated in cell adhesion-mediated drug resistance (33,34). In a previous report, CD49d was not found on BM resident stromal cells (32), and there is a single report describing its presence on MVs (35). Primarily, we confirmed our mass spectrometry observation that CD49d is elevated in MM-MSCs MVs compared to ND-MSCs MVs by FACS (n = 13) (Figure 3a). We registered higher percentages of MM-MSCs MVs with detectable CD49d (average 80% versus 30%, $P < 0.05$) and higher mean levels of CD49d per cell (3.7 MFI versus 2 MFI, $P < 0.05$) compared to ND-MSCs MVs. Next, we assessed whether the increased CD49d expression on the MM-MSCs MVs is conveyed to MM cells upon uptake by testing MM cell lines with and without exposure to the MVs (24 h) for their CD49d expression (MFI, FACS). Increased expression of CD49d was registered in MM cell lines treated with MM-MSCs MVs (↑40%, $P < 0.01$), yet no change MM cells treated with ND-MSCs MVs (Figure 3b). We also tested whether CD49d increased in MM cells treated with MM-MSCs MVs when protein synthesis was inhibited (cycloheximide). Results showed that elevated CD49d in recipient cells was partially attributed to its transfer from the MVs (↑20–25%, $P < 0.05$) (Figure 3b).

Having established that CD49d is indeed transferred from the MM-MSCs MVs to MM cells, we explored its participation in the MVs uptake (Figure 3c). We applied the monoclonal anti CD49d antibody natalizumab (NTZ, Tysabri) clinically used in multiple sclerosis (36) to MM cells cultured with PKH67 stained BM-MSCs

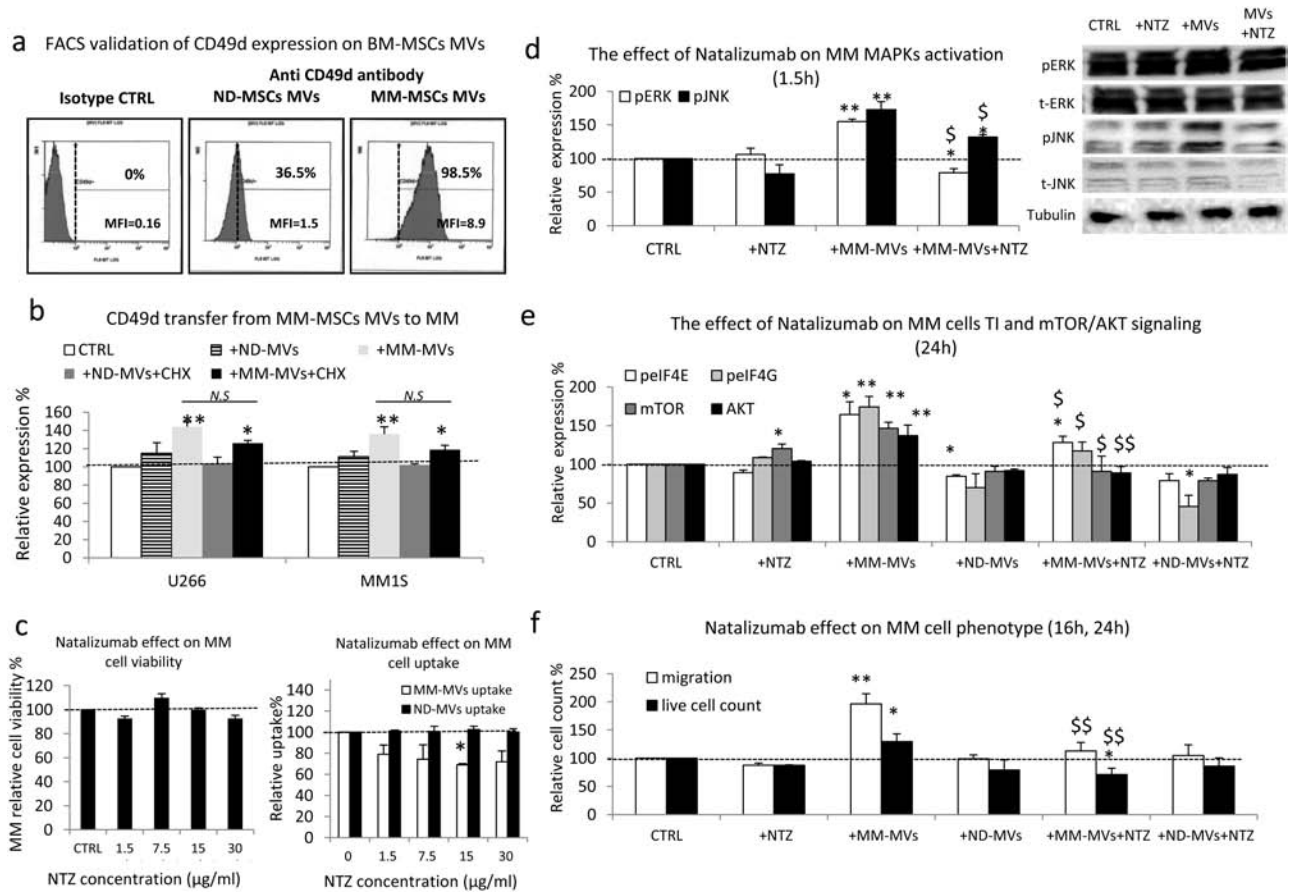

Figure 3. The delivery of CD49d from the MM-MSCs to MM cells by the MVs and the inhibitory effect of Natalizumab on MM signaling and phenotype: (**a**) BM-MSCs MVs (ND/MM) were incubated with anti CD49d APC antibody, and the CD49d expression was assayed by FACS. (**b**) CD49d transfer from BM-MSCs (ND, MM) to MM cells (U266 and MM1S) was tested by FACS 24 h after MM cells treatment with MSCs MVs using anti CD49d antibody. (**c**) The MM cells viability and BM-MSCs MVs uptake into MM cells was measured 24 h after Natalizumab (NTZ) treatment (0–30 µg). Relative MFI (mean fluorescence intensity) was measured by FACs. (**d, e**) U266 cells were co-treated with MM-MSCs' MVs with or without NTZ (15 µg). Protein lysates were extracted and assayed for (d) MAPKs: p/t ERK, p/t JNK, (e) peIF4E, p eIF4GI, mTOR, and AKT. Results expressed as percent (mean ± SE, $n \geq 3$) of respective protein expression in control cells not treated with MVs and NTZ (dotted line). All immunoblots were quantified and normalized for tubulin. (**f**) The effect of MM-MSCs MVs on U266 MM cells live cell count (trypan blue) migration (transwell assay) with or without NTZ (15 µg) was tested after 24 h and 16 h respectively. (d–f) additional *t*-tests were performed between MM cells treated with MVs only or combined with drugs ($ $P < 0.05$, $$ $P < 0.01$). Asterisks depict statistical significance (*$P < 0.05$, **$P < 0.01$).

MVs (ND, MM) and tested MVs uptake by FACS. We registered decreased levels of MM-MSCs MVs PKH67 MFI in MM cells treated with NTZ (15 µg/ml) (↓30% MFI, $P < 0.05$) but no change in the uptake of ND-MSCs MVs (Figure 3c). There was no difference in the percentage of MM-MSCs MVs positive cells with NTZ suggesting NTZ was able to limit uptake rate per cell but enabled a certain extent of uptake into all cells (data not shown). In concordance with decreased MVs uptake in the presence of NTZ and perhaps impediment of CD49d membranal signaling there was complete abrogation of the MM-MSCs MVs stimulation of MAPKS/TI signaling in recipient MM cells (↓50–80%, $P < 0.05$) (Figure 3d, e). Since CD49d is known for stimulating Akt/mTOR-dependent signaling (37), we also tested the effect of NTZ on this cascade in our model and again observed significant attenuation (↓40–50%, $P < 0.01$) (Figure 3e). As expected, the NTZ reduced MAPKs/TI signaling (1.5 h–24 h) resulted in complete inhibition of the MM-MSCs MVs stimulated MM cell proliferation and migration (16 h) (↓60% and ↓100%, respectively; $P < 0.05$) (Figure 3f). Importantly, the effect of NTZ on MM cells' proliferation/death was considered in the assessment of cells' migration. Specifically, death was irrelevant since the MM cells did not die in response to NTZ (data not shown, there was no effect on cells' viability (Figure 3c) and nor significant change in live cell count (Figure 3f, black bars). Thus, the measurement of decreased migration was analyzed as is and determined as significantly compromised upon NTZ treatment (15 µ g/ml) (Figure 3f, white bars). Moreover, the lack of any NTZ effect on ND-MSCs MVs treated MM cells (uptake, signaling, phenotype) suggests that its action is contingent on the CD49-enriched MVs (MM-MSCs' MVs only).

Natalizumab resensitizes MM-MSCs MVs treated MM cells to bortezomib and doxorubicin

Accumulating data suggest that MVs can instill drug resistance in cancer cells (11). Therefore, the inhibition of MVs uptake should eliminate their protection. We explored this approach in our model and demonstrated that indeed MM-MSCs MVs afford protection to MM cells (U266, MM1S) from doxorubicin (Dox) and bortezomib (Vel) (↑25%, $P < 0.05$) (Figure 4a). More importantly, NTZ was able to completely cancel this effect and re-sensitize the MM cells to the drugs (Figure 4a). Interestingly, NTZ had no effect on uptake of ND-MSCs MVs and consequent changes in recipient cells (in parameters we observed) lending specificity to our strategy. Based on these results, we addressed MM-MSCs MVs only in the next steps of our studies.

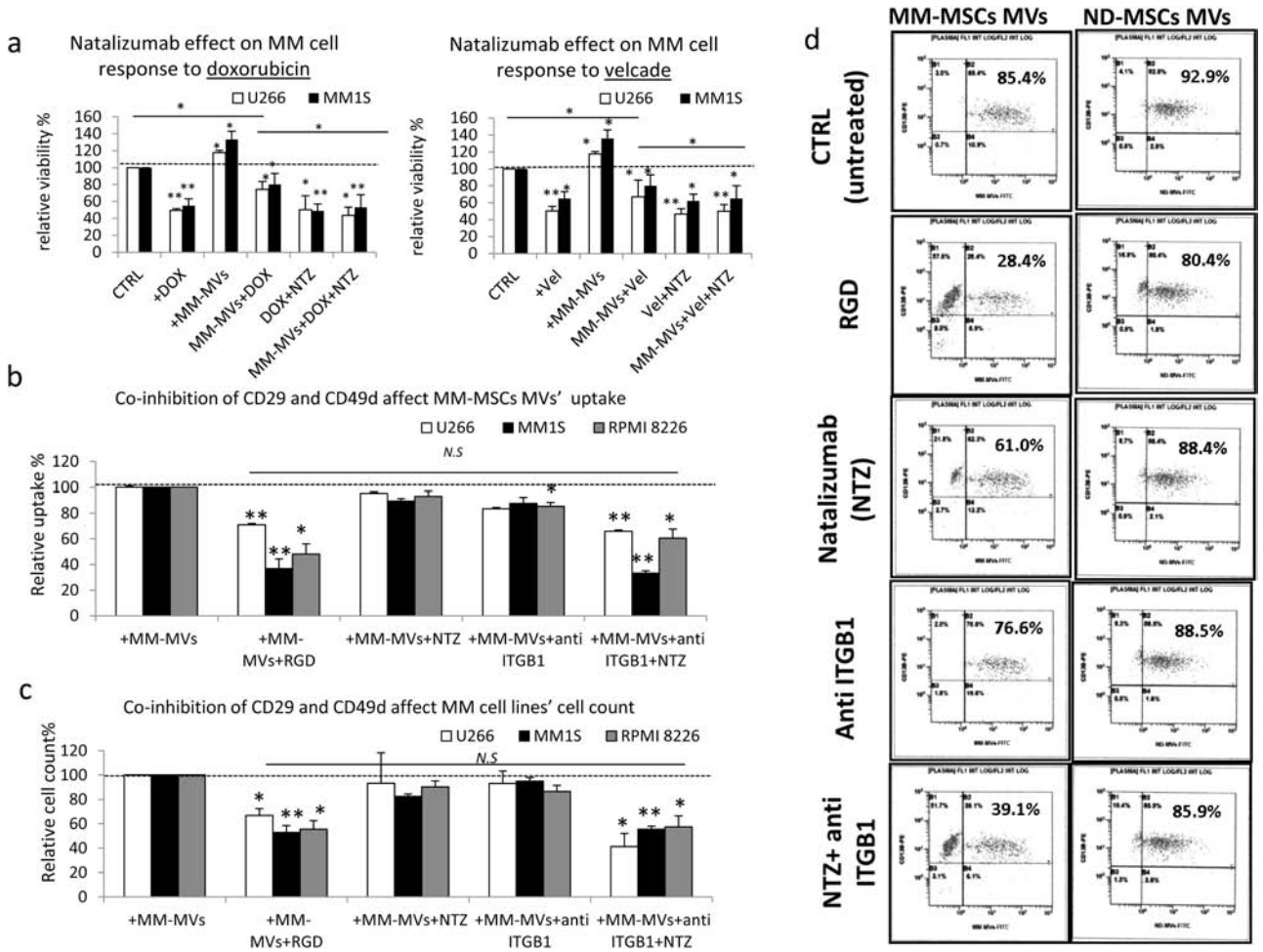

Figure 4. Natalizumab sensitized the MM cells to MM drugs, and combination with anti CD29 inhibits MM-MSCs' MVs uptake and their effect on MM cells' proliferation: (**a**) U266 and MM1S cells were co-treated with the anti-MM drugs Velcade (5 nM) or doxorubicin (1 μM) with MM-MSCs MVs and NTZ (15 μg) and cell viability was measured (WST1). Results expressed as percent (mean ± SE, $n \geq 3$) of relative viability compare control cells not treated with MVs and NTZ (dotted line). (**b**) MM-MSCs MVs uptake into MM cells (U266, RPMI8226 and MM1S) was measured 24 h after treating with NTZ (15 μg/ml) and anti ITGB1 (10 μg/ml). Graphs data represent the relative uptake (FACs). (**c**) The effect of MM-MSCs MVs on U266 MM cells' (U266, RPMI8226, and MM1S) live cell count (trypan blue) without natalizumab/anti CD29 was tested after 24 h. Results expressed as percent (mean ± SE, $n \geq 3$) of relative uptake/live cell count compared to control cells not treated with the inhibitors (dotted line). Asterisks depict statistical significance (*$P < 0.05$, **$P < 0.01$). (**d**) ND/MM-MSCs MVs uptake into primary PCs was measured 24 h after treating with RGD, NTZ (15 μg/ml), and anti ITGB1 (10μg/ml). The graphs figure represent the relative uptake (FACs).

ITGB1 cooperates with CD49d to control the MM-MSCs MVs communication with MM cells

Our inability to completely block the RGD-dependent integrins mediated MM-MSCs MVs uptake with NTZ promoted us to evaluate the involvement of its natural partner the CD29 (integrin β1) also elevated in MM-MSCs MVs compared to ND-MSCs MVs according to the mass spectrometry analysis (×2 folds). We simultaneously co-applied an inhibitory anti ITGB1 antibody, NTZ, and BM-MSCs MVs (ND, MM) to MM cells (U266, MM1S, RPMI8226) and recorded the uptake of the MVs (% positive cells and MFI). We observed the inhibition of MM-MSCs MVs uptake equal to RGD but no effect on the uptake of ND-MSCs MVs (↓36–65%, $P < 0.01$) (Figure 4b). Importantly, NTZ and anti ITGB1 antibody had no effect on MM cells live counts (data not shown). These results indicate that VLA4 (CD49d/CD29) is responsible for the RGD-dependent uptake of MM-MSCs MVs into MM cells. Here too, we demonstrated that once MM-MSCs MVs uptake was blocked with ITGB1 blocker and NTZ there was reduced proliferation equivalent to RGD's influence (Figure 4c). Lastly, in order to establish the relevance of this strategy to MM patients, we tested the uptake inhibitors (RGD, ITGB1 blocker, and NTZ effect on primary plasma cells (PCs) treated with ND/MM-MSCs MVs. We measured PKH67 dyed ND/MM-MSCs MVs' uptake after a 24-h incubation. Results demonstrated again that the RGD/NTZ/ITGB1 inhibitor/and combination selectively inhibited MM-MSCs MVs uptake into PCs without effecting the ND-MSCs MVs internalization.

MM-MSCs MVs' CD49d expression is positively correlated with MM staging and predicts poorer response to therapy

Since we have shown that MM cells' CD49d is transferred from surrounding MM-MSCs' MVs and affects MM cells' phenotype/signaling we wondered whether there is any evidence of its clinical relevance, that is, disease staging and response to treatment. Therefore, we compared the levels of CD49d on MM-MSCs' MVs at diagnosis and before any treatment in a panel of SMM/MM patients ($n = 31$) with their clinical history and laboratory

Table 1. Gene ontology (GO) analyses of the cargo protein lists in BM-MSCs MVs according to source

	ToppGene	Webgestalt	GOrilla
ND MSCs MVs			
Cellular response to stimuli			
Cellular oxidant detoxification	9.41E-11	1.59E-08	
Response to chemical stimulus		1.82E-07	
Response to biotic stimulus	1.787E-08	1.61E-07	7.19E-04
Response to stress		2.51E-07	
Response to oxidative stress	1.64E-06		
Response to reactive oxygen species	1.333E-07		
Immune response			
Regulation of immune system process	3.87E-20	3.46E-08	6.70E-04
Lymphocyte co-stimulation			6.50E-05
Neutrophil degranulation	2.92E-38	2.92E-10	
Immune response	2.87E-20		3.86E-04
Immune system process		2.99E-10	
Antigen processing and presentation	5.98E-03	1.87E-17	
ECM organization and binding			
Positive regulation of cell-cell adhesion			1.96E-04
Extracellular matrix organization	5.88E-06		
Integrin signaling pathway	2.81E-06		
ECM-receptor interaction	1.15E-05		
Integrin cell surface interactions	1.58E-06		
Protein binding		5.10E-03	
Receptor binding		4.04E-03	
Co-enzyme binding		4.00E-04	
Focal adhesion	4.00E-05		
Cell adhesion molecule binding	3.61E-05		2.75E-06
Vesicles and uptake			
Cytoplasmic membrane-bounded vesicle		2.61E-09	
Membrane-bounded vesicle		5.10E-35	
Vesicles mediated transport		2.48E-34	
Phagocytosis	6.02E-06		
Transport vesicle membrane			2.70E-04
MM MSCs MVs			
Translation			
Translation	3.02E-32	2.28E-46	1.21E-07
Metabolism of proteins	1.03E-09	1.12E-45	8.91E-06
Translation termination	3.02E-37	1.75E-30	
Translation elongation	2.42E-37	3.49E-28	
Ribosome	2.83E-30	3.59E-27	8.79E-11
Translation initiation	1.64E-36	1.45E-30	9.51E-08
Cap-dependent translation initiation	1.64E-36	1.75E-30	
Protein targeting and immune response			
Protein targeting	2.91E-15	1.56E-28	5.11E-06
Protein targeting to membrane	1.07E-24	2.04E-28	1.61E-07
Co-translational protein targeting to membrane	2.04E-28	2.04E-28	9.51E-08
Antigen processing and presentation	3.01E-06	1.91E-11	
PD-1 signaling	3.01E-08		
CTL-mediated immune response against target cells	3.01E-04		

characteristics (Supplementary Table 1, available at *Carcinogenesis* Online). We observed a positive correlation between MSCs MVs' CD49d mean fluorescence intensity (MFI) and the levels of free light chain (FLC) ($R = 0.7204$, $P < 0.01$) (Figure 5a). Consistent with correlation to FLC, there was also a positive correlation between CD49d expressing MVs (%) and percentage of the plasma cells in the BM of SMM/MM patients ($R = 0.5308$) (Figure 5b). We also determined elevated CD49d expression (% and MFI) in MM-MSCs MVs of MM patients at advanced disease stages (stages 2 and 3 versus stage 1, according to the International Scoring System -ISS staging ($P < 0.05$), which integrates the levels of albumin and β 2 microglobulin measured in the patients' blood samples (38) (Figure 5c). Finally, we observed that patients with higher levels of BM-MSCs' MVs' CD49d expression at diagnosis have reduced probabilities to achieve complete remission, whereas patients with lower CD49d achieved complete remission or very good partial response ($P < 0.05$) (Figure 5d) (Supplementary Table 2, available at *Carcinogenesis* Online).

Discussion

The role of MVs in intercellular communication is unfolding at a rapid pace with much data attesting to significant participation in cancer (10,11,39). The systemic dispersion of MVs underlies their great involvement in cancer microenvironment design, potential as cancer markers and intricate participation in cellular

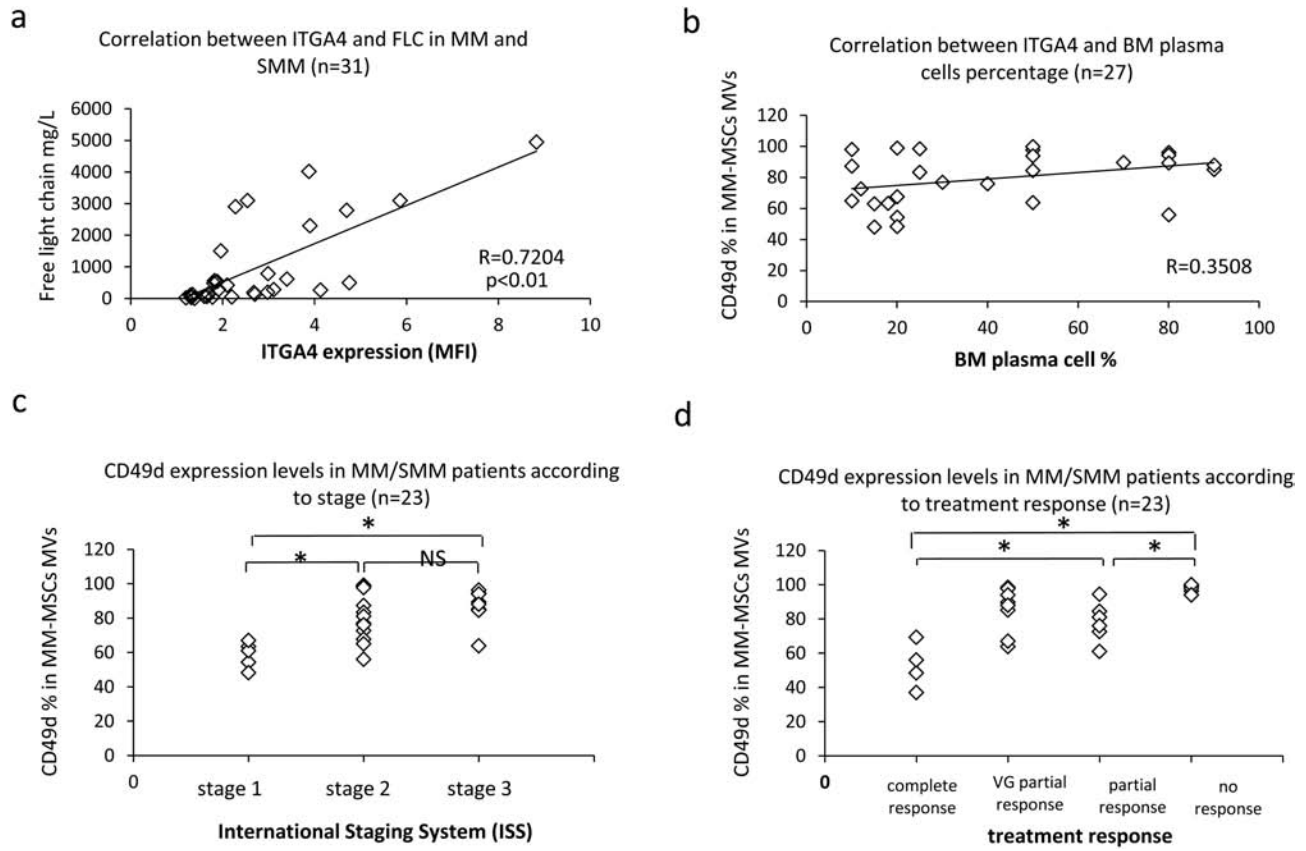

Figure 5. MM-MSCs MVs' CD49d expression is positively correlated with MM staging and predicts poorer response to therapy. CD49d expression levels in the BM-MSCs MVs of 31 MM/MGUS/SMM patient was tested at the day of the diagnosis, and the correlation with the FLC (**a**), BM plasma cells % (**b**), stage of the disease (**c**), and treatment response (**d**) were tested. The correlation between CD49d and the MM clinical markers in 31 MM patients was performed using Pearson or Spearman's rho correlations for normal or non-normal distributions, respectively. Tests of normality were performed for all the MM clinical markers data using Kolmogorov–Smirnov and Shapiro–Wilk tests. Asterisks depict statistical significance (*$P < 0.05$, **$P < 0.01$).

functions such as proliferation, migration, and drug resistance (10,11). Previously, we have shown that BM-MSCs and MM cells maintain a dynamic and crucial dialogue partially attributed to MVs (7,8). The mission ahead was to identify the specific signals that generate the MVs procancer activity and conceive ways to intervene. Concordantly, we characterized the ND-MSCs and MM-MSCs' MVs protein cargoes (proteomes) and determined differences according to normal or pathological source. By focusing on molecules differentially expressed, we identified a means to control the MVs uptake via inhibition of integrin partners CD49d and CD29. To the best of our knowledge, this is the first demonstration of a selective way to prevent the uptake of cancer promoting MVs (MM-MSCs MVs) while retaining the uptake of cancer suppressing MVs (ND-MSCs MVs) (7,8).

This is particularly interesting in light of the natural equal uptake rates of BM-MSCs MVs from either source (ND, MM). In consideration of this conundrum it is imperative to note that while ND-MSCs MVs express lower levels of CD49d they also express higher levels of other integrins that may facilitate the MVs uptake by different signaling pathways (Supplementary Table 1, available at *Carcinogenesis* Online). It is also well established that several mechanisms are at play in MVs internalization not necessarily contingent on integrins at all. It will be interesting to explore this issue further in the future.

Integrins are principal mediators of MM association with the BM microenvironment's cellular and noncellular components, particularly stromal cells and extracellular matrix (40). Interactions prompted by integrins contribute to the survival, proliferation, migration, and drug resistance of MM cells (40). Moreover, it is well recognized that VLA4 participates in these signals in MM where it binds fibronectin (FN) and VEGF and is overexpressed on drug resistant cells (33,40). VLA4 is expressed differentially on MM cell lines and can be increased via inside-out signaling of HGF or cytokines (40). Our study has shown that CD49d may also be elevated via horizontal transfer of the integrin from one cell type to another with MVs, namely, the BM-MSCs to MM cell lines. This was described previously with integrins expressed on exosomes in another cell system but not with MVs, VLA4 specifically, or in BM-MSCs/MM interactions (41).

A previous study showed that direct inhibition of CD49d diminished MM stimulation by BM stroma *in vitro* and in a mouse model (42). Here, we expanded this observation from the recognized ligands of CD49d (FN, VEGF, IGF, etc.) to include an additional layer in the dialogue with the cell surroundings, that is, the systemic MM-MSCs MVs. We demonstrated that inhibition of CD49d was capable of attenuating the procancer signals instigated by MM-MSCs MVs. Moreover, our results (current and previous (8)) indicate that the MM-MSCs MVs signaling is comprised by two stages: the contact and the uptake and delivery of cargo. By blocking the contact both steps of communication are abrogated. In fact, additional preliminary observations in ongoing studies we are performing underscore a possible mechanism for the MM-MSCs MVs cargo to increase recipient MM cells protein

translation (unpublished data). Despite the recognition that the BM stroma is actively involved in the malignant process, there is a paucity of microenvironmental markers in clinical use (43–45). Based on our findings, we decided to examine the relevance of the CD49d expression on MM-MSCs MVs (%, MFI) cultured *in vitro* to clinical characteristics of the patients and their response to treatment. Interestingly, we observed a positive correlation between CD49d levels (MFI) and FLC and more importantly to the accepted ISS staging. The biological relevance of this observation is further accentuated by the capability of CD49d levels on BM-MSCs of MM patients at diagnosis to predict the patients' response to treatment. The capacity of CD49d to predict drug response and consequently survival was also demonstrated in CLL (46). Previous studies depict CD49d as an independent marker underscoring its importance and unique biological context. To the best of our knowledge, this is the first report of a marker present on constituents in the BM microenvironment that are actively transferred to the MM cells and have biological relevance to disease markers.

Our final and crucial evidence demonstrates that VLA4 facilitates the uptake of the MVs. More importantly, despite its presence on both ND-MSCs MVs and MM-MSCs MVs its inhibition prevented the uptake of the latter only. Indeed, it may be argued that the elevated levels of CD49d on the MVs from MM-MSCs dictated its novel function, for instance by integrin clustering (47–49). A previous study reported that endothelial progenitor cells derived MVs were incorporated in endothelial cells by binding VLA4 on the MVs membranes (50). Indeed the participation of integrins in endocytosis and phagocytosis is established (51), and we have already shown previously that BM-MSCs MVs uptake into the MM cells involves both processes (8). There is also evidence that EVs interact with ECM and integrins (52). Interestingly and to the best of our knowledge, this is the first evidence that vesicles' uptake may be controlled by a specific integrin, thereby demonstrating new levels of selectivity. Additional studies are required to determine the VLA4 receptor on the recipient MM cells, which may be other integrins, ICAM and so on (53) and possibly serve as therapeutic targets as well.

The full capacity of RGD to inhibit the MM-MSCs MVs uptake and signaling in MM cells was only realized by us when we also inhibited the CD49d beta chain partner, the ITGB1 (CD29). This is unsurprising since integrins function in complex and VLA4 expression is correlated with cancer progression (41). It is well established that a 1:1 ratio of alpha and beta subunits compose of the integrins. Yet, we registered unequal respective elevations (X80 and X2) of CD49d and ITGB1 on MM-MSCs' MVs compared to ND-MSCs MVs. This may be reconciled with the mass spectrophotometry information regarding the actual quantity of each protein that indicated closer concentrations of both proteins (3:1, data not shown). Importantly, NTZ did not display significant anti-MM activity when applied to the MM cells in the absence of the MM-MSCs MVs. This observation is particularly important in light of an incomplete and terminated clinical trial with NTZ in relapsed and refractory myeloma that did not yield any results due to low enrolment (https://clinicaltrials.gov/ct2/show/NCT00675428). Furthermore, this clinical study enrolled refractory MM patients and our observations demonstrate the importance of CD49d in early stages of the disease. On the contrary, we have shown here that CD49d/VLA4 inhibition is effective at negating the supportive involvement of the BM microenvironment and therefore may be beneficial when applied in concert with other MM therapies and in cases of developed drug resistance. Uniquely, the observation that MM-MSCs MVs' CD49d expression is correlated with disease progression affords the first marker for the microenvironment. We put forward that future studies should address its potential to mark the disease progression from pre-malignant MGUS to full blown MM. Ongoing studies by us are aimed at assessing this approach with the hope of improving the monitoring of MM development and maybe designing means to prevent its transformation from unsymptomatic MGUS to the fatal MM. We are also looking into the contribution of additional differentially expressed proteins on the MM-MSCs MVs to MM cells with the intent of uncovering more support mechanisms provided by the cancer surroundings and new disease markers and therapeutic targets.

The inhibition of CD49d is a partial inhibition; as we described in the manuscript NTZ does not affect the cells viability but can inhibit the MVs mediated interaction between the MM cells and the MM-MSCs. In addition, NTZ and anti-ITGB1 treatments at the specified work concentrations did not have significant effects on healthy BM-MSCs. This result may indicate the specific activity of the inhibitors on the malignant microenvironment without affecting the healthy one. In summary, this study underscores the differential role of MVs according to their cargo/source in the communication between the malignant cells and their microenvironment. The results presented here demonstrate that selective inhibition of the MVs uptake/signaling is possible and holds great potential in canceling out the BM afforded support of MM. Finally, this study uncovered the role of CD49d in intercellular communication and highlights its importance in conveying the MSCs procancer activity.

Ethical approval

All participants signed informed consent forms approved by Meir Medical Center Helsinki Committee. Consent for publication: Not applicable. Datasets of proteomics analyses and other material related to the current study are readily available upon request.

Supplementary material

Supplementary data are available at *Carcinogenesis* online.

Funding

This work was supported by the Cancer Biology Research Center (CBRC) (#0601242482) Dream Idea Grant, Dotan Hemato-Oncology seed award 2017, Tel Aviv University, and the Takeda Israel LTD Prize. The study presentation costs were supported by the Israel Ministry of Science, Technology and Space.

Acknowledgements

The study was performed in partial fulfillment of the requirements for a Ph.D. degree by Dabbah Mahmoud, Sackler Faculty of Medicine, Tel Aviv University, Tel Aviv, Israel. We are grateful to the staff of the Hematocytological Laboratory for its dedicated technical support, the orthopedics and hematologists for their willing participation in collection of samples at Meir Medical Center, Kfar Saba, Israel.
Conflict of Interest Statement: None declared.

References

1. Röllig, C. *et al.* (2015) Multiple myeloma. *Lancet*, 385, 2197–2208.
2. Palumbo, A. *et al.* (2011) Multiple myeloma. *N. Engl. J. Med.*, 364, 1046–1060.
3. Alzrigat, M. *et al.* (2018) Epigenetics in multiple myeloma: from mechanisms to therapy. *Semin. Cancer Biol.*, 51, 101–115.

4. Go, R.S. *et al.* (2018) How I manage monoclonal gammopathy of undetermined significance. *Blood*, 131, 163–173.
5. Manier, S. *et al.* (2012) Bone marrow microenvironment in multiple myeloma progression. *J. Biomed. Biotechnol.*, 2012, 157496.
6. Kawano, Y. *et al.* (2015) Targeting the bone marrow microenvironment in multiple myeloma. *Immunol. Rev.*, 263, 160–172.
7. Attar-Schneider, O. *et al.* (2016) Multiple myeloma and bone marrow mesenchymal stem cells' crosstalk: effect on translation initiation. *Mol. Carcinog.*, 55, 1343–1354.
8. Dabbah, M. *et al.* (2017) Microvesicles derived from normal and multiple myeloma bone marrow mesenchymal stem cells differentially modulate myeloma cells' phenotype and translation initiation. *Carcinogenesis*, 38, 708–716.
9. Marcus, H. *et al.* (2016) Mesenchymal stem cells secretomes' affect multiple myeloma translation initiation. *Cell. Signal.*, 28, 620–630.
10. Ciardiello, C. *et al.* (2016) Focus on extracellular vesicles: new frontiers of cell-to-cell communication in cancer. *Int. J. Mol. Sci.*, 17, 175.
11. Wendler, F. *et al.* (2017) Extracellular vesicles swarm the cancer microenvironment: from tumor-stroma communication to drug intervention. *Oncogene*, 36, 877–884.
12. D'Souza-Schorey, C. *et al.* (2012) Tumor-derived microvesicles: shedding light on novel microenvironment modulators and prospective cancer biomarkers. *Genes Dev.*, 26, 1287–1299.
13. EL Andaloussi, S. *et al.* (2013) Extracellular vesicles: biology and emerging therapeutic opportunities. *Nat. Rev. Drug Discov.*, 12, 347–57.
14. Wendler, F. *et al.* (2017) Extracellular vesicles swarm the cancer microenvironment: from tumor-stroma communication to drug intervention. *Oncogene*, 36, 877–884.
15. Ohyashiki, J.H. *et al.* (2018) Extracellular vesicle-mediated cell-cell communication in haematological neoplasms. *Philos. Trans. R. Soc. Lond. B. Biol Sci.*, 373, 20160484.
16. Dabbah, M. *et al.* (2016) Multiple myeloma cells promote migration of bone marrow mesenchymal stem cells by altering their translation initiation. *J. Leukoc. Biol.*, 100, 761–770.
17. Attar-Schneider, O. *et al.* (2016) Multiple myeloma and bone marrow mesenchymal stem cells' crosstalk: effect on translation initiation. *Mol. Carcinogen.*, 55, 1343–1354.
18. Attar-Schneider, O. *et al.* (2016) Secretome of human bone marrow mesenchymal stem cells: an emerging player in lung cancer progression and mechanisms of translation initiation. *Tumour Biol.*, 37, 4755–4765.
19. Tyanova, S. *et al.* (2016) The Perseus computational platform for comprehensive analysis of (prote)omics data. *Nat. Methods*, 13, 731–740.
20. Eden, E. *et al.* (2009) GOrilla: a tool for discovery and visualization of enriched GO terms in ranked gene lists. *BMC Bioinformatics*, 10, 48.
21. Chen, J. *et al.* (2009) ToppGene Suite for gene list enrichment analysis and candidate gene prioritization. *Nucleic Acids Res.*, 37, W305–W311.
22. Wang, J. *et al.* (2013) WEB-based GEne SeT AnaLysis Toolkit (WebGestalt): update 2013. *Nucleic Acids Res.*, 41, W77–W83.
23. Huang, d.a.W. *et al.* (2009) Systematic and integrative analysis of large gene lists using DAVID bioinformatics resources. *Nat. Protoc.*, 4, 44–57.
24. Epstein Shochet, G. *et al.* (2017) First trimester human placenta prevents breast cancer cell attachment to the matrix: the role of extracellular matrix. *Mol. Carcinogen.*, 56, 62–74.
25. Zafar, H. *et al.* (2017) αIIbβ3 binding to a fibrinogen fragment lacking the γ-chain dodecapeptide is activation dependent and EDTA inducible. *Blood Adv.*, 1, 417–428.
26. Zismanov, V. *et al.* (2015) Multiple myeloma proteostasis can be targeted via translation initiation factor eIF4E. *Int. J. Oncol.*, 46, 860–870.
27. Ciobotaro, P. *et al.* (2003) The effects of doxorubicin on apoptosis and adhesion molecules of normal peripheral blood leukocytes-an ex vivo study. *Anticancer Drugs*, 14, 383–389.
28. Zhang, H., *et al.* (2017) ClC5 decreases the sensitivity of multiple myeloma cells to Bortezomib via promoting pro-survival autophagy. *Oncol. Res.*, 26, 421–429.
29. Moschos, S.J., *et al.* (2007) Integrins and cancer. *Oncology (Williston Park)*, 21, 13–20.
30. Doherty, G.J. *et al.* (2009) Mechanisms of endocytosis. *Annu. Rev. Biochem.*, 78, 857–902.
31. Kapp, T.G. *et al.* (2013) Integrin modulators: a patent review. *Expert Opin. Ther. Pat.*, 23, 1273–1295.
32. Paiva, B. *et al.*; Spanish Myeloma Group/Program for the Study of Malignant Blood Diseases Therapeutics (GEM / PETHEMA) Cooperative Study Groups. (2016) Phenotypic and genomic analysis of multiple myeloma minimal residual disease tumor cells: a new model to understand chemoresistance. *Blood*, 127, 1896–1906.
33. Noborio-Hatano, K. *et al.* (2009) Bortezomib overcomes cell-adhesion-mediated drug resistance through downregulation of VLA-4 expression in multiple myeloma. *Oncogene*, 28, 231–242.
34. Podar, K. *et al.* (2011) The selective adhesion molecule inhibitor Natalizumab decreases multiple myeloma cell growth in the bone marrow microenvironment: therapeutic implications. *Br. J. Haematol.*, 155, 438–448.
35. Nomura, S. *et al.* (2008) Alpha 4-integrin-positive microvesicles and SDF-1 in peripheral blood stem cell harvest. *Bone Marrow Transplant.*, 41, 1071–1072.
36. Brandstadter, R. *et al.* (2017) The use of natalizumab for multiple sclerosis. *Neuropsychiatr. Dis. Treat.*, 13, 1691–1702.
37. Kim, I.D. *et al.* (2017) Osteopontin peptide icosamer containing RGD and SLAYGLR motifs enhances the motility and phagocytic activity of microglia. *Exp. Neurobiol.*, 26, 339–349.
38. Palumbo, A. *et al.* (2015) Revised international staging system for multiple myeloma: a report from international myeloma working group. *J. Clin. Oncol.*, 33, 2863–2869.
39. Moore, C. *et al.* (2017) The emerging role of exosome and microvesicle-(EMV-) based cancer therapeutics and immunotherapy. *Int. J. Cancer*, 141, 428–436.
40. Katz, B.Z. (2010) Adhesion molecules – the lifelines of multiple myeloma cells. *Semin. Cancer Biol.*, 20, 186–195.
41. Paolillo, M.A.-O., and Schinelli, S. (2017) Integrins and exosomes, a dangerous liaison in cancer progression. *Cancers (Basel)*, 9, E95.
42. Podar, K. *et al.* (2011) The selective adhesion molecule inhibitor Natalizumab decreases multiple myeloma cell growth in the bone marrow microenvironment: therapeutic implications. *Br. J. Haematol.*, 155, 438–448.
43. Bolomsky, A. *et al.* (2017) IKAROS expression in distinct bone marrow cell populations as a candidate biomarker for outcome with lenalidomide-dexamethasone therapy in multiple myeloma. *Am. J. Hematol.*, 92, 269–278.
44. Pojero, F. *et al.* (2015) Old and new immunophenotypic markers in multiple myeloma for discrimination of responding and relapsing patients: the importance of "normal" residual plasma cell analysis. *Cytometry B. Clin. Cytom.*, 88, 165–182.
45. Himani, B. *et al.* (2016) Ki-67 immunostaining and its correlation with microvessel density in patients with multiple myeloma. *Asian Pac. J. Cancer Prev.*, 17, 2559–2564.
46. Bulian, P., *et al.* (2014). CD49d is the strongest flow cytometry-based predictor of overall survival in chronic lymphocytic leukemia. *J. Clin. Oncol.*, 32(9), 897–904.
47. Grabovsky, V. *et al.* (2000) Subsecond induction of alpha4 integrin clustering by immobilized chemokines stimulates leukocyte tethering and rolling on endothelial vascular cell adhesion molecule 1 under flow conditions. *J. Exp. Med.*, 192, 495–506.
48. Isberg, R.R. *et al.* (2000) Signaling and invasin-promoted uptake via integrin receptors. *Microbes Infect.*, 2, 793–801.
49. Werner, E. (2005) Integrin clustering drives phagocytosis coupled to collagenase 1 induction through RhoA GTPase and superoxide production. *Antioxid. Redox Signal.*, 7, 318–326.
50. Deregibus, M.C. *et al.* (2007) Endothelial progenitor cell derived microvesicles activate an angiogenic program in endothelial cells by a horizontal transfer of mRNA. *Blood*, 110, 2440–2448.
51. Sayedyahossein, S. *et al.* (2013) Integrins and small GTPases as modulators of phagocytosis. *Int. Rev. Cell Mol. Biol.*, 302, 321–354.
52. Maas, S.L.N. *et al.* (2017) Extracellular vesicles: unique intercellular delivery vehicles. *Trends Cell Biol.*, 27, 172–188.
53. French, K.C. *et al.* (2017) Extracellular vesicle docking at the cellular port: extracellular vesicle binding and uptake. *Semin. Cell Dev. Biol.*, 67, 48–55.